



## On-chip DNA preconcentration in different media conductivities by electrodeless dielectrophoresis

Shunbo Li,<sup>1,2</sup> Ziran Ye,<sup>1</sup> Yu Sanna Hui,<sup>1</sup> Yibo Gao,<sup>3</sup> Yusheng Jiang,<sup>4</sup> and Weijia Wen<sup>1,3,a)</sup>

<sup>1</sup>*Department of Physics and Nano Science and Technology Program, The Hong Kong University of Science and Technology, Clear Water Bay, Kowloon, Hong Kong*

<sup>2</sup>*School of Chemistry, University of Leeds, Woodhouse Lane, Leeds LS2 9JT, United Kingdom*

<sup>3</sup>*Environmental Science Program, The Hong Kong University of Science and Technology, Clear Water Bay, Kowloon, Hong Kong*

<sup>4</sup>*College of Communication Engineering, Chongqing University, Chongqing 400044, China*

(Received 13 August 2015; accepted 21 September 2015; published online 30 September 2015)

Electrodeless dielectrophoresis is the best choice to achieve preconcentration of nanoparticles and biomolecules due to its simple, robust, and easy implementation. We designed a simple chip with microchannels and nano-slits in between and then studied the trapping of DNA in high conductive medium and low conductive medium, corresponding to positive and negative dielectrophoresis (DEP), respectively. It is very important to investigate the trapping in media with different conductivities since one always has to deal with the sample solutions with different conductivities. The trapping process was analyzed by the fluorescent intensity changes. The results showed that DNA could be trapped at the nano-slit in both high and low conductive media in a lower electric field strength (10 V/cm) compared to the existing methods. This is a significant improvement to suppress the Joule heating effect in DEP related experiments. Our work may give insight to researchers for DNA trapping by a simple and low cost device in the Lab-on-a-Chip system.  
© 2015 AIP Publishing LLC. [<http://dx.doi.org/10.1063/1.4932177>]

### I. INTRODUCTION

The demand for on-chip biomolecule detection and analysis<sup>1</sup> increases as the biomedical devices evolve and integrate into miniaturized analytical systems. Fundamentally, biomolecule analysis is limited by detection limit because of the small sample volume. On-chip preconcentration has become the most favourable approach against this problem. DNA, as a common biomolecule, is an important entity in complex samples, such as blood, saliva, and cytoplasm and its dynamics in miniaturized systems has been studied extensively.<sup>2,3</sup> It is widely used in forensic, medical diagnostics, and evolutionary studies.<sup>4,5</sup> Therefore, developing a simple, portable, reusable, and low-cost device<sup>6,7</sup> to enrich DNA is highly desirable in bio-information analysis.<sup>8</sup>

Direct filtration of DNA by nanofilter<sup>9</sup> from a large amount of sample solution is regarded as the most straightforward method to enrich the DNA concentration. However, it is too specific for DNA molecules with a certain length due to its fixed pore size. Chemical method,<sup>10,11</sup> based on absorption and desorption processes, is another conventional way to enhance DNA concentration, prior to capillary electrophoresis (EP). Electrical method is the most popular technique due to its simple implementation and reliability. But it is difficult to integrate for on-chip applications.

A number of researchers demonstrated on-chip DNA trapping by constructing charged membranes such as poly-AMPS 2-acrylamido-2-methyl-1-propanesulfonic acid,<sup>12</sup> polyacrylamide

<sup>a)</sup> Author to whom correspondence should be addressed. Electronic mail: [phwen@ust.hk](mailto:phwen@ust.hk). Tel.: 852 2358 7979. Fax: 852 2358 1652.

membranes,<sup>13</sup> polyimide,<sup>14</sup> and Nafion<sup>15</sup> in microchannels. However, the drawback of charged membrane is the change of the ionic charges in the surrounding buffer solutions, and such kind of device is not applicable for mass production. Manipulation of small quantities of DNA by electric field induced forces in confined channels seems to be gaining its popularity as an important technique in molecular biology. Electroosmosis (EO) and EP effects were usually applied for concentrating DNA. Hsieh *et al.*<sup>16</sup> presented an enhancement of DNA at the interface of poly (ethylene oxide) (PEO) and (tris)-borate (TB) buffers. Dai *et al.*<sup>17</sup> demonstrated DNA preconcentration based on the balance of EO and EP. It is based on the fact that the velocities of EO and EP are opposite for DNA, inducing an enhancement of DNA concentration at the location where the velocities of EO and EP are of the same magnitude. Stein *et al.*<sup>18</sup> found DNA aggregation in nanochannels by using similar method of force balancing. However, it is very difficult to create a condition in which EO mobility and EP mobility are exactly identical in magnitude. Furthermore, EO is greatly related to the ion concentration of buffer solution<sup>19</sup> and such technique is commonly adapted in low conductivity medium. Electrodeless dielectrophoresis (EDEP), which requires small constriction to generate large DEP force, is the best candidate to trap DNA in medium with a wide range of conductivities. Simulation work on electrokinetics and dielectrophoresis was reported in which it trapped nanoscale biomolecules in physiological media of high conductivity.<sup>20</sup> Recently, Chia-Fu Chou's group demonstrated the trapping of protein and DNA by nano-constriction.<sup>21–23</sup> The requirements of time-consuming fabrication of nano-constriction (e.g., ebeam lithography) and the high electric field strength are inevitable.

This paper aimed to make the chip preparation simpler and lower down the electric field to minimize the Joule heating effect, as well as testing the chip in different sample solutions with different conductivities. The main content of this work include: introduce a new simple and effective device in Section II, discuss the mechanisms (electrodeless dielectrophoresis, electric field analysis of size effect, and Ogston sieving trapping mechanism) behind this experiment in Sections III and IV A, monitor the influence of electroosmotic flow in solutions with different conductivity and trap DNA in these corresponding solutions by positive DEP and negative DEP in Sections IV B and IV C.

## II. EXPERIMENTAL TECHNIQUES

A schematic diagram depicting the basic fabrication process is shown in Fig. 1. It consists of two parts: channel fabrication and preparation of polydimethylsiloxane (PDMS) thin film for bonding. Photolithography, dry etching, and photoresist stripping are the basic processes for constructing silicon channels. First, a silicon wafer was cleaned in  $\text{H}_2\text{SO}_4\text{:H}_2\text{O}_2$  solution (volume ratio of 10:1) at 120 °C for 10 min, followed by rinsing in deionized (DI) water,  $\text{HF:H}_2\text{O}$  solution (1:50) for 1 min and DI water again for 4 cycles, and spin-dried in hot  $\text{N}_2$  gas for 15 min. Then the Si wafer was coated by hexamethyldisiloxane (HMDS) to enhance the adhesion between wafer and photoresist. Photoresist HPR 504 was spin coated at 4000 rpm for 30 s. The wafer was transferred to Mask Aligner (SUSS Microtec MA6–2, Garching, Germany) for exposure, followed by developing in FHD-5 for 60 s and post-baked on a hot plate at 120 °C for 60 s. The Si wafer was then etched by a DRIE machine (Surface Technology systems, Newport, United Kingdom) and photoresist stripping in PS210 Photoresist Asher (PVA Tepla AG, Kirchheim, Germany) was then conducted for 25 min to form the nanochannel. The same steps were carried out to define the microchannel with aligned photolithography. Thermal oxide of 10 nm thickness was grown using a diffusion furnace to insulate the channels and prevent current leakage. The preparation of PDMS thin film involved pouring PDMS onto a silanized silicon wafer and covering it by a glass slide with inlets and outlets holes. After curing at 60 °C for 2 h, the glass slide with thin film was peeled off and holes on PDMS were punched. The last step was the sealing of the channel by as-prepared PDMS thin film. No plasma treatment is required in this fabrication method.<sup>19</sup> Thus, it could be reused for many times after proper cleaning. The fabricated device was also shown at the lower right corner of Fig. 1. It has two reservoirs for inlets and two for outlets. The channel area is outlined by red-dashed line.

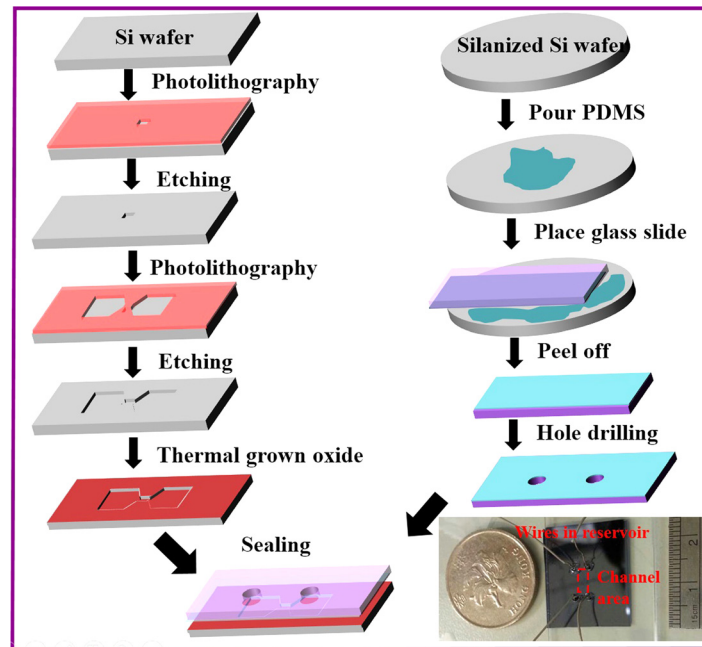


FIG. 1. A schematic diagram showing the fabrication process for nanofluidic chip with two microchannels and a nano-slit in between. The inset at the lower right corner is the real picture of fabricated device which has four reservoirs for inlets and outlets.

The layout of the fabricated microchannel was shown in Fig. 2. Both optical and AFM images clearly showed the morphology of the fabricated microchannels and the dimension of the nano-slits. Fig. 2(a) is the optical image showing two microchannels and nano-slits. The inset is the enlarged picture for one set of microchannel and nano-slit. Figs. 2(b)–2(d) are the

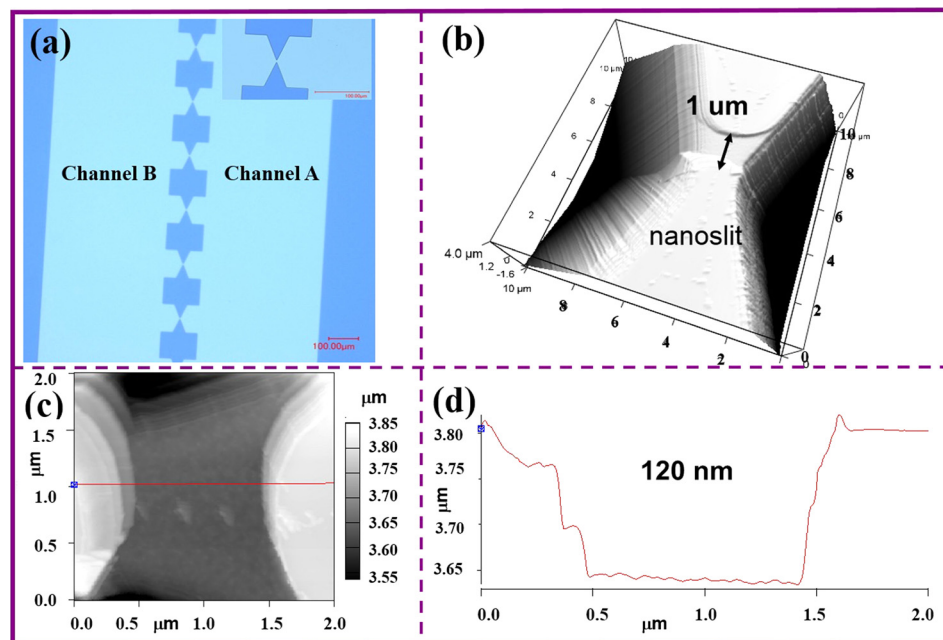


FIG. 2. Illustration of nanofluidic device for DNA trapping: (a) the optical image of channel layout consists of two microchannels and nano-slits in between. The inset is the enlarged picture for one unit; (b) the 3D image of nano-slit with the size of  $1\ \mu\text{m}$ . Picture is taken by AFM; (c) the 2D image of the slit and (d) the height profile of the red line in (c).

AFM images: 2(b) is the 3D image showing a nano-slit with the lateral size of  $1\ \mu\text{m}$ , 2(c) is the 2D image of the nano-slit, and 2(d) the height profile of the red line in 2(c). There are two microchannels—A and B which are connected by a thin junction whose width was about  $1\ \mu\text{m}$  and depth was about  $120\ \text{nm}$ . The junction serves to suppress the electric field across the nano-slit. When biomolecules are passing through the nano-slit, they experience very large DEP force. The width of nano-slit is limited by the photolithography process and ebeam lithography has to be used for smaller size. The trapping effect is known as Ogston sieving and exhibits when the size of the junction is larger than the size of DNA.

DNA fragments with length of 2k bp obtained by collecting DNA marker after electrophoresis were chosen as a sample biomolecule. The suspending media were TB-EDTA (TBE) buffer and NaCl solutions, which were prepared at a concentration of  $0.5\times$  and  $500\ \text{mM}$ , respectively. The  $500\ \text{mM}$  NaCl solution will result in a solution with conductivity over  $1\ \text{S/m}$ . The  $0.5\times$  working solution is  $45\ \text{mM}$  tris-borate (weight ratio tris base: borate acid = 2:1) plus  $1\ \text{mM}$  EDTA. Rhodamine B (Sigma Aldrich, USA) was added to the solutions for characterizing electroosmotic flow. In order to visualize DNA in the solution, SYBR-Green (Invitrogen, Carlsbad, CA, USA) was added to the solution with a concentration of  $0.01\%$ . DC power supply was used to provide an external electric field for DNA manipulation. COMSOL 4.3 was used to analyze the electric field distribution when electrical signal was applied. The fluorescent intensities were obtained by Matlab (version 2008b, MathWorks, Natick, MA, USA).

### III. THEORY

#### A. Electrodeless dielectrophoresis

We first discuss the background of the mechanism in the electrodeless dielectrophoresis. Dielectric particles will experience the electrokinetic effect including EO and EP in DC electric field. The electrokinetic velocity could be expressed as<sup>24</sup>

$$\bar{u}_{EK} = \mu_{EK} \bar{E} = (\mu_{EO} - \mu_{EP}) \bar{E} = \frac{\varepsilon_m (\zeta_P - \zeta_w)}{\eta} \bar{E}, \quad (3.1)$$

where  $\bar{u}_{EK}$  is the electrokinetic velocity,  $\mu_{EK}$  is the electrokinetic mobility,  $\varepsilon_m$  is the permittivity of the suspending medium,  $\zeta_P$  and  $\zeta_w$  are the zeta-potentials of the particle and channel wall,  $\eta$  is the dynamic viscosity of the solution, and  $\bar{E}$  is the electric field applied.

It is clearly seen that direction of electrophoretic mobility dominates the resultant net movement of flow if electrophoretic mobility is larger than the electroosmotic mobility, and vice versa.

When dielectric particle with spherical shape is presented in the non-uniform electric field, it will experience the so-called DEP force. The time averaged DEP force could be written as

$$\bar{F}_{DEP} = 2\pi\varepsilon_m a^3 f_{CM} \nabla |\bar{E}|^2, \quad (3.2)$$

where  $a$  is the radius of particle and  $f_{CM}$  is the Clausius-Mossotti factor (CM factor), which could be expressed as

$$f_{CM} = (\sigma_p - \sigma_m) / (\sigma_p + 2\sigma_m), \quad (3.3)$$

where  $\sigma_p$  and  $\sigma_m$  are the electric conductivities of particle and medium, respectively. If the particle is less conductive than the suspending medium, the CM factor is negative. Then it is called negative DEP (n-DEP), meaning particles will be repelled from the high electric field. On the other hand, if particle is more conductive than the medium, particles will be attracted to the high electric field, meaning positive DEP (p-DEP).

## B. Simulation of the electric field distribution

The electric field gradients near the nano-slit is an important feature in DEP related experiments. In order to analyze the size effect of nano-slit, COMSOL simulation was performed. The electric field distribution and related DEP forces are illustrated in Fig. 3. The size of large channel where DNA travels is  $100\text{ }\mu\text{m}$  which has the same size as the device structure. The left figure (Fig. 3(a)) shows the constriction of  $10\text{ }\mu\text{m}$  while the figure on the right (Fig. 3(b)) shows the  $1\text{ }\mu\text{m}$  wide constriction. It is clear that electric field concentrates at the junction and the field intensifies when the channel size shrinks 10 times. For the case of Fig. 3(b), the electric field was largely enhanced when the junction was 1% of the big channel. The DEP force which corresponds to the gradient of electric field intensity is also plotted in the same figure. The results indicate that the smaller the junction, the larger the DEP force which decreases gradually away from the junction. This is a comparison to show the enhancement of electric field and DEP force. One can imagine how high it could be in the vertical direction when the size goes further down to near  $100\text{ nm}$ . The size effect on DEP force magnitude can therefore be concluded that DEP force can be enhanced with small junctioned nano-slit which in turn improved the DNA trapping percentage.

Biomolecules such as DNA and protein have relatively small sizes (less than  $100\text{ nm}$ ) while cells are in the order of microns. The electric field effect such as DEP force in biomolecules is not as strong as that among organic or inorganic nanoparticles. Therefore, there exists a challenge of manipulating biomolecules by field effects. One approach is to design a device with a structural dimension comparable to biomolecules. According to the simulation results presented in this paper, it is evident that the DEP force can be enhanced with the reduction of junction size in the device for trapping DNA.

## IV. RESULTS AND DISCUSSION

### A. Verification of trapping mechanism

Electromigration of polyelectrolytes (e.g., DNA and proteins) in confined space could be divided into three groups:<sup>25</sup> (1) Ogston sieving, the radius of gyration of molecule ( $R_g$ ) is smaller than the pore size  $a$ ; (2) Entropic trapping,  $R_g \approx a$ ; and (3) Biased reptation,  $R_g > a$ . The physical mechanisms of these three types are different. Experiments were performed to confirm the trapping mechanism of DNA molecules in our device and the results are shown in Fig. 4. DNA with size of  $2000\text{ bp}$  was dispersed in  $0.5\times\text{TBE}$  buffer before they were injected into channel A. DNA quickly diffused and moved to channel B if no electric signal was applied (Fig. 4(a)). However, DNA cannot pass through nanojunctions when an electric signal of  $5\text{ V}$  was applied (Fig. 4(b)). This is because DNA would experience large steric hindrance originates from DEP force which confirms the trapping mechanism is Ogston sieving.

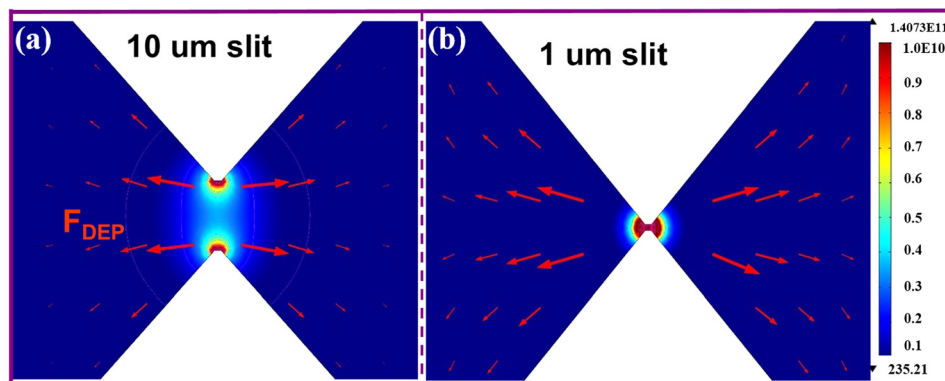


FIG. 3. Comparison of electric field distribution near the junctions of different sizes: (a) channel size shrinks from  $100\text{ }\mu\text{m}$  to  $10\text{ }\mu\text{m}$  and (b) channel size shrinks from  $100\text{ }\mu\text{m}$  to  $1\text{ }\mu\text{m}$ . The strength of the electric field is indicated by color bar on the right of the figure. Electric field is most intense at the junction. The red arrows indicate the direction and magnitude of DEP force.



In the following sections [IV B](#) and [IV C](#), we will investigate the trapping efficiency when different buffer solutions with various conductivities are used.

## B. DNA trapping in high conductive medium

The pre-concentration process is governed by three phenomena—EP, EO, and DEP. All of them are influenced by the surrounding medium limited by the effective electrical double layer. In our work, the size of the channel is in the order of nanometer which gives rise to a relatively strong electroosmotic effect. The EO flow is initiated from the positive potential to the negative potential within the  $\text{SiO}_2$  channel. In contrast, DNA molecules migrate from the negative end to the positive end because DNA is negatively charged. As a result, the impact of EO flow against the electrophoretic flow of DNA was investigated. Fluorescent dye—rhodamine B was used as a tracer for the EO flow. Fig. 5 shows the electroosmotic flow of 500 mM NaCl and  $0.5 \times$  TBE solution from channel A to channel B, which depicts that EO flow is very slow process and it has almost no effect on the electrophoresis process of DNA in this highly conductive ( $>1$  S/m) sample solution.

DNA trapping process was also conducted with high conductivity buffer solutions. It is noted that the voltage applied for DNA trapping is inverted compared to EO experiment in Fig. 5. It is based on the assumption that channel A (right one) is the inlet for sample injection and channel B (left one) is the outlet. In order to monitor the EO flow and DNA trapping from channel A to channel B based on the fact EO and EP have opposite directions, the voltages applied in EO experiment and DNA trapping have opposite directions. Actually, the device in this experiment has symmetrical structure. The voltage applied from left to right could be reversed. It all depends on the channel where sample solution is injected. Assuming the whole trapping effect is only governed by electrophoresis and dielectrophoresis, we performed DNA harvesting on our device using solution containing 500 mM NaCl and  $0.5 \times$  TBE which results in a conductivity over 1 S/m. This is a high conductive solution usually used to mimic the situation in blood (similar conductivity to physiological media<sup>26</sup>). Some cells are suspended in this kind of high conductive solution and could be lysed to release DNA for detection and analyzing. The prepared solution was introduced in channel A and electric signal of 5 V was applied, inducing an electric field of 10 V/cm across the channel. Fig. 6 shows the trapping process of DNA with low concentration. Initially, DNA molecules were uniformly dispersed in the buffer solution. The density of DNA molecules increases rapidly at the nano-slit over the time, meaning the concentration of DNA at the nano-slit is relatively higher than the region away from nano-slit. For simplicity of estimating the increment

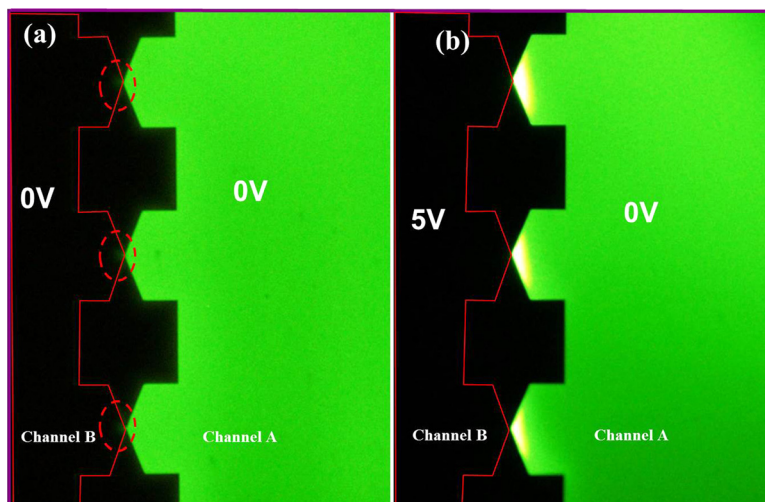


FIG. 4. The trapping mechanism of DNA near the nano-slit: (a) the diffusion of DNA from one channel (A) to another (B) without applied electric field and (b) the trapping of DNA fragments after applying electric signal of 5 V for 1 min. The buffer solution used was  $0.5 \times$  TBE buffer.

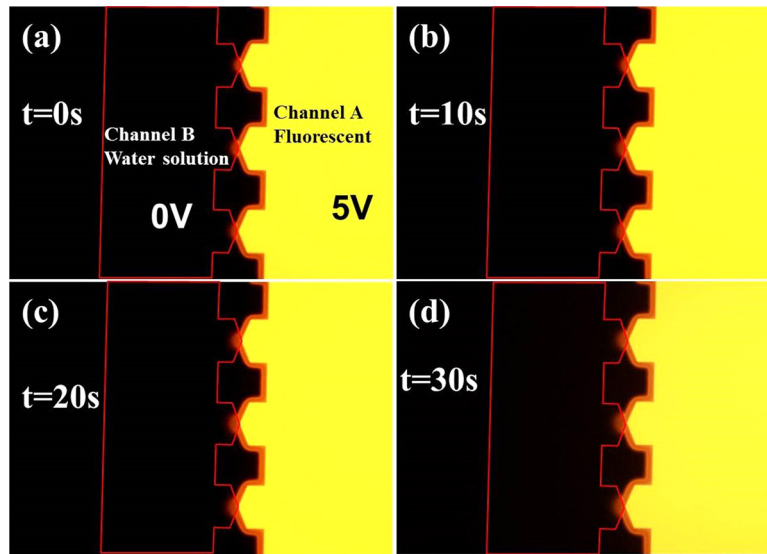


FIG. 5. The electroosmotic effect between channels A and B when applied voltage was 5 V. The solution used in this experiment was rhodamine B in 500 mM NaCl and  $0.5\times$  TBE solution (channel A).

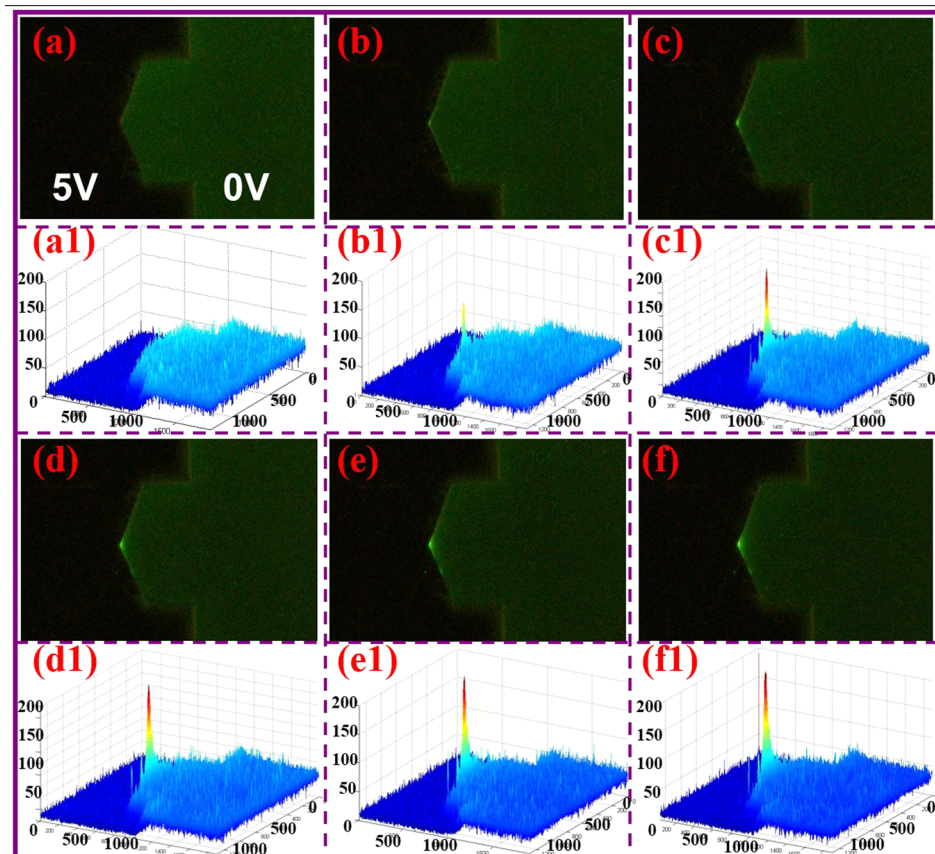


FIG. 6. DNA trapping at the nano-slit when electric signal of 5 V (10 V/cm) was applied. (a)–(f) The fluorescent images captured at a time interval of 5 s and (a1)–(f1) is the change in fluorescent intensity after extracting the information from (a)–(f) by Matlab. The buffer solution used is 500 mM NaCl and  $0.5\times$  TBE. The X and Y axes is the pixel corresponding to the real picture and Z axis is the fluorescent intensity.

of DNA concentration, the fluorescent intensity was extracted in Fig. 6. It indicated that the concentration was magnified near 5 times in 10 s. Compared to in-line preconcentration method<sup>11</sup> (100 times in 40 min) and on-chip polymerase chain reaction (PCR)<sup>27</sup> (40 cycles in 108 min), the proposed method is quick enough to increase DNA concentration for analytic and detection purpose.

It is noted that the preconcentration of DNA in this high conductive solution is achieved by p-DEP. In order to confirm this p-DEP phenomenon, we reversed the direction of electric field after trapping DNA for 20 s and we can still see a bright spot near the nano-slit. Positive DEP means the particles will be attracted at the point with highest electric field gradient (near the nano-slit in this experiment) and reversion of electric field direction cannot move DNA from the nano-slit due to the large p-DEP attraction force. On the other hand, DNA will be totally released if it is governed by n-DEP force which is a repelling force and no driving force (EP force is reversed to be the same direction of repelling force) is existed after reversing the direction of electric field. This phenomenon is consistent with the previous works in high conductive medium.<sup>28</sup> It is also seen that DNA aggregates very near the nano-slit, thus the p-DEP mechanism is verified again.

### C. DNA trapping in low conductive medium

What might happen if we decrease the conductivity of the buffer solution by decreasing the concentration of solute? In this scenario, the electroosmotic flow is relatively high because EO mobility is proportional to Zeta potential which will be enhanced if ion concentration decreases.  $0.5\times$  TBE buffer solution with and without fluorescent dye were injected into channel A and channel B, respectively. Then, an electric signal of 5 V was applied and the whole process was recorded by CCD camera. Fig. 7 shows the time lapse of EO flow through channel A to channel B when the potential of the reservoir of channel A was set to 5 V while the reservoir of channel B was grounded. It is clearly seen that fluid flows quickly from channel A to channel B, evidencing the existence of EO flow. The EO flow rate was calculated to be 2.51 pl/s according to our previous method by monitoring the fluorescent intensity change.<sup>19</sup> In comparison to Fig. 5, the EO flow showed significant enhancement in Fig. 7.

The trapping process was recorded over time. Fig. 8 illustrated the accumulation of DNA at a time interval of 5 s. When electric field exhibits in the channel, DNA molecules move

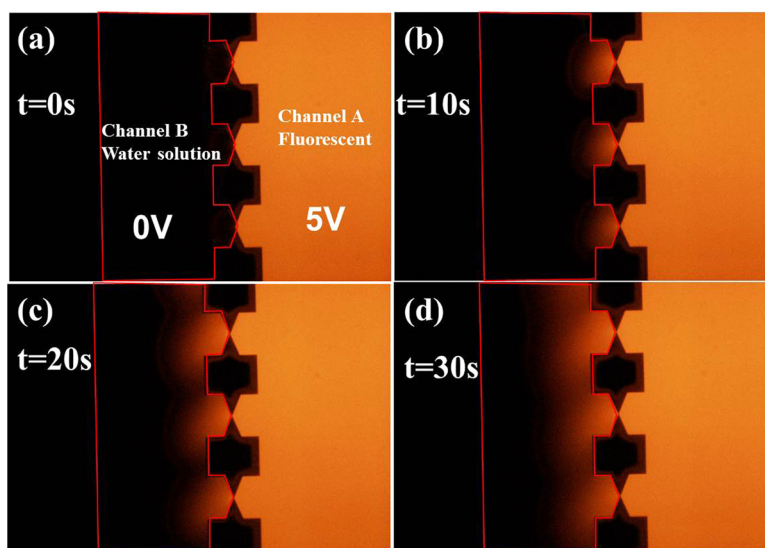


FIG. 7. The electroosmotic effect observed when applied voltage was 5 V. The EO flow rate was 2.51 pl/s. The solution used in this experiment was rhodamine B dissolved in  $0.5\times$  TBE buffer solution (channel A).



along the field lines. As soon as the DNA reaches the nano-slit, it experiences large negative DEP force due to the abrupt change in channel structure. DNA molecules are unable to pass through the nano-slit and thus accumulated near the slit, leading to an increase in DNA concentration and fluorescent intensity at the slit as the time goes on. The observations suggest that our device could operate under high electroosmotic flow, and one can conclude that electrophoretic effect is greater than the electroosmotic effect. In this case of low conductive medium, DNA experiences negative DEP force. Comparing Figs. 8 and 6, the accumulation of DNA is faster in Fig. 8 (the bright green area is larger while the intensity is almost the same) which is coherent with the fact that DNA moves faster in low conductive solutions, meaning the harvesting is faster in buffer solution with low conductivity. Unlike the p-DEP phenomenon in high conductive medium, the bright spots will disappear after reversing the direction of electric field, indicating it is governed by n-DEP.

After performing DNA trapping in solutions with different concentrations using our nano device, one may conclude that the preconcentration of DNA can be conducted with a wide range of conductivity of running solutions regardless of the magnitude of EO flow which is quite large in our case. Other researchers could achieve a 5 orders magnification of DNA concentration in 1000 s by using nanofracture method.<sup>14</sup> However, the applied voltage in their experiment was 300 V. In our case, although the preconcentration factor was not so high (5–7 times in 10 s according to the fluorescent intensity change in Figs. 6 and 8), the applied voltage was only 5 V (10 V/cm). It could greatly suppress the Joule heating effect and make the device more stable. In addition, the proposed design could perform continuous trapping of DNA by

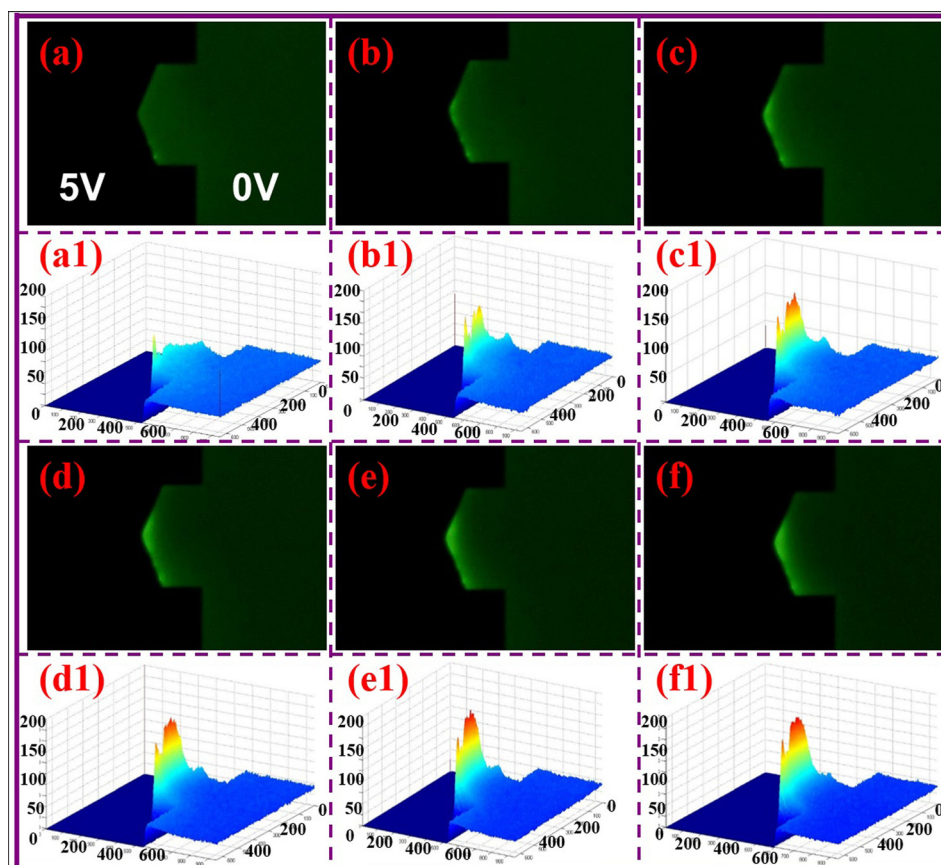


FIG. 8. DNA trapping at nano-slit when electric signal of 5 V (10 V/cm) was applied. (a)–(f) The fluorescent images captured at a time interval of 5 s and (a1)–(f1) is the change in fluorescent intensity after extracting the information from (a) to (f) by Matlab. The buffer solution used is  $0.5\times$  TBE. The X and Y axes is the pixel corresponding to the real picture and Z axis is the fluorescent intensity.

both p-DEP in high conductive medium and n-DEP in low conductive medium: the applied electric field would drive DNA to the nano-slit and capture it while sample solutions flow in channel A with a certain flow rate. The concentrated solution could be extracted after a certain time for further analysis.

## V. CONCLUSIONS AND OUTLOOKS

In this work, DNA trapping under different medium conductivities was investigated in an electrodeless nanofluidic chip. This whole process involves EP, EO, and DEP effects. Both EP and EO forces are affected by the medium conductivity, especially their directions are opposite. We designed a nano-slit structure and confirmed its possibility of trapping DNA by numerical simulation. The EO velocity was monitored prior to DNA trapping in the same medium. High conductive medium had very low EO velocity and it would have almost no effect on preventing DNA trapping. Our results also showed that DNA could be trapped at the nano-slit as well even when EO effect is high in low conductive medium. Thus, this design is applicable in miniaturized system which has to deal with a large variety of samples with different conductivities. Compared to other existing techniques, this device and method has advantages in four points: (1) It is simple and low cost in fabrication. Ebeam lithography and anodic bonding are usually required to prepare 2D nano-constrains. We demonstrated a chip with 1D nano-slit (no ebeam lithography) and PDMS bonding is good enough to achieve on-chip capturing of DNA. (2) It could operate in a wide range of solution conductivity and trapping could be achieved by both positive and negative DEP. This also confirmed that the EO flow do not affect the performance of trapping efficiency in this proposed device. People always face different solutions with a wide range of conductivity. However, very few of the preconcentration method consider this situation. (3) Relatively low electric field (10 V/cm) was used. This is favourable for on-chip electrochemical process since the Joule heating effect is minimized in this case. (4) It could operate in continuous manner, which means one can collect the high concentrated solution after running for a certain time (e.g. 20 mins).

Unlike DNA and proteins which have relatively large gyration sizes, other biomarkers such as peptides are difficult to concentrate by DEP method due to the small induced dipoles resulting in small DEP forces. In this case, ion-selective membrane<sup>29</sup> and granules<sup>30</sup> are regarded as the more advantageous technology to concentrate them for further analysis. In general, ion-selective membrane and granules are suitable for on-chip preconcentrating small charged molecules and DEP method is good for on-chip preconcentrating large biomolecules (e.g., DNA and proteins) in which large dipoles could be induced by external electric field. On the other hand, although membrane method is easy and low cost, excess washing step is required for membrane preparation in microfluidic chips. However, DEP based microfluidic devices especially for our device with 1D nano-slit structures has another advantage of large scale integration for lab-on-a-chip device since most of these fabrication methods are based on planar microfabrication.<sup>31</sup> Thus, one can choose the best method for their own applications according to the fabrication facilities and the target entities.

## ACKNOWLEDGMENTS

The authors would like to thank Mr. Weipeng Zhang from Environmental Science Program, HKUST for providing DNA and the fruitful discussions. The authors acknowledge the financial support provided by the Hong Kong Research Grants Council (Grant Nos. HKUST604710 and 605411) and National Natural Science Foundation of China (Grant No. 11290165). This work was partially supported by Award No. SA-C0040/UK-C0016 made by King Abdullah University of Science and Technology (KAUST).

<sup>1</sup>I.-F. Cheng, H.-L. Yang, C.-C. Chung, and H.-C. Chang, *Analyst* **138**, 4656 (2013).

<sup>2</sup>J. O. Hardin and V. T. Milam, *Soft Matter* **7**, 2674 (2011).

<sup>3</sup>D. J. Mai, C. Brockman, and C. M. Schroeder, *Soft Matter* **8**, 10560 (2012).

<sup>4</sup>S.-J. Park, T. A. Taton, and C. A. Mirkin, *Science* **295**, 651 (2002).

<sup>5</sup>T. G. Drummond, M. G. Hill, and J. K. Barton, *Nat. Biotechnol.* **21**, 1192 (2003).

- <sup>6</sup>J. Khandurina, T. E. McKnight, S. C. Jacobson, L. C. Waters, R. S. Foote, and J. M. Ramsey, *Anal. Chem.* **72**, 2995 (2000).
- <sup>7</sup>P.-A. Auroux, Y. Koc, A. deMello, A. Manz, and P. J. R. Day, *Lab Chip* **4**, 534 (2004).
- <sup>8</sup>A. Estevez-Torres and D. Baiql, *Soft Matter* **7**, 6746 (2011).
- <sup>9</sup>I. Vlassiuk, A. Krasnoslobodtsev, S. Smirnov, and M. Germann, *Langmuir* **20**, 9913 (2004).
- <sup>10</sup>A. Wainright, U. T. Nguyen, T. Bjornson, and T. D. Boone, *Electrophoresis* **24**, 3784 (2003).
- <sup>11</sup>A. Feng, N. T. Tran, C. Chen, J. Hu, M. Taverna, and P. Zhou, *Electrophoresis* **32**, 1623 (2011).
- <sup>12</sup>H. Kim, J. Kim, E.-G. Kim, A. J. Heinz, S. Kwon, and H. Chun, *Biomicrofluidics* **4**, 043014 (2010).
- <sup>13</sup>R. J. Meagher and N. Thaitrong, *Electrophoresis* **33**, 1236 (2012).
- <sup>14</sup>Z.-Y. Wu, C.-Y. Li, X.-L. Guo, B. Li, D.-W. Zhang, Y. Xu, and F. Fang, *Lab Chip* **12**, 3408 (2012).
- <sup>15</sup>D.-W. Zhang, H.-Q. Zhang, L. Tian, L. Wang, F. Fang, K. Liu, and Z.-Y. Wu, *Microfluid. Nanofluid.* **14**, 69 (2013).
- <sup>16</sup>M.-M. Hsieh, W.-L. Tseng, and H.-T. Chang, *Electrophoresis* **21**, 2904 (2000).
- <sup>17</sup>J. Dai, T. Ito, L. Sun, and R. M. Crooks, *J. Am. Chem. Soc.* **125**, 13026 (2003).
- <sup>18</sup>D. Stein, Z. Deurvorst, F. H. J. van der Heyden, W. J. A. Koopmans, A. Gabel, and C. Dekker, *Nano Lett.* **10**, 765 (2010).
- <sup>19</sup>S. Li, W. Cao, Y. S. Hui, and W. Wen, *Nanoscale Res. Lett.* **9**, 147 (2014).
- <sup>20</sup>V. Chaurey, C. Polanco, C.-F. Chou, and N. S. Swami, *Biomicrofluidics* **6**, 012806 (2012).
- <sup>21</sup>N. Swami, C.-F. Chou, V. Ramamurthy, and V. Chaurey, *Lab Chip* **9**, 3212 (2009).
- <sup>22</sup>K.-T. Liao, M. Tsegaye, V. Chaurey, C.-F. Chou, and N. S. Swami, *Electrophoresis* **33**, 1958 (2012).
- <sup>23</sup>V. Chaurey, A. Rohanl, Y.-H. Su, K.-T. Liao, C.-F. Chou, and N. S. Swami, *Electrophoresis* **34**, 1097 (2013).
- <sup>24</sup>R. Pethig, *Biomicrofluidics* **4**, 022811 (2010).
- <sup>25</sup>J. Fu, J. Yoo, and J. Han, *Phys. Rev. Lett.* **97**, 018103 (2006).
- <sup>26</sup>S. Park, Y. Zhang, T.-H. Wang, and S. Yang, *Lab Chip* **11**, 2893 (2011).
- <sup>27</sup>N. R. Beer, B. J. Hindson, E. K. Wheeler, S. B. Hall, K. A. Rose, I. M. Kennedy, and B. W. Colston, *Anal. Chem.* **79**, 8471 (2007).
- <sup>28</sup>L. Ying, S. S. White, A. Bruckbauer, L. Meadows, Y. E. Korchev, and D. Klenerman, *Biophys. J.* **86**, 1018 (2004).
- <sup>29</sup>T. Leichlé and C.-F. Chou, *Biomicrofluidics* **9**, 034103 (2015).
- <sup>30</sup>H.-P. Chen, C.-C. Tsai, H.-M. Lee, S.-C. Wang, and H.-C. Chang, *Biomicrofluidics* **7**, 044110 (2013).
- <sup>31</sup>Z. Slouka, S. Senapati, and H.-C. Chang, *Annu. Rev. Anal. Chem.* **7**, 317–335 (2014).